Dual modes of rabies P-protein association with microtubules: a novel strategy to suppress the antiviral response

Gregory W. Moseley[1,*], Xavier Lahaye[2], Daniela M. Roth[1], Sibil Oksayan[1], Richard P. Filmer[1], Caitlin L. Rowe[1], Danielle Blondel[2] and David A. Jans[1]

[1]Nuclear Signalling Laboratory, Department of Biochemistry and Molecular Biology, Monash University, Clayton, Victoria 3800, Australia
[2]Laboratoire de Virologie Moléculaire et Structurale, UMR-CNRS 2472/UMR-INRA 1157, CNRS, Allée de la terrasse, 91198 Gif sur Yvette, France
*Author for correspondence (greg.moseley@med.monash.edu.au)

Accepted 20 July 2009
Journal of Cell Science 122, 3652-3662 Published by The Company of Biologists 2009
doi:10.1242/jcs.045542

Summary

Conventional nuclear import is independent of the cytoskeleton, but recent data have shown that the import of specific proteins can be either facilitated or inhibited by microtubules (MTs). Nuclear import of the P-protein from rabies virus involves a MT-facilitated mechanism, but here, we show that P-protein is unique in that it also undergoes MT-inhibited import, with the mode of MT-interaction being regulated by the oligomeric state of the P-protein. This is the first demonstration that a protein can utilise both MT-inhibited and MT-facilitated import mechanisms, and can switch between these different modes of MT interaction to regulate its nuclear trafficking. Importantly, we show that the P-protein exploits MT-dependent mechanisms to manipulate host cell processes by switching the import of the interferon-activated transcription factor STAT1 from a conventional to a MT-inhibited mechanism. This prevents STAT1 nuclear import and signalling in response to interferon, which is vital to the host innate antiviral response. This is the first report of MT involvement in the viral subversion of interferon signalling that is central to virus pathogenicity, and identifies novel targets for the development of antiviral drugs or attenuated viruses for vaccine applications.

Supplementary material available online at
http://jcs.biologists.org/cgi/content/full/122/20/3652/DC1

Key words: Interferon, Microtubules, Nuclear trafficking, Rabies virus

Introduction

Nucleocytoplasmic trafficking of transcription factors is a central mechanism in cellular processes such as development and innate immunity (Gardner and Montminy, 2005; Jans et al., 2000; Pemberton and Paschal, 2005; Poon and Jans, 2005; Randall and Goodbourn, 2008; Reich and Liu, 2006; Ziegler and Ghosh, 2005). Conventionally, protein nuclear trafficking involves the interaction of nuclear localisation sequences (NLSs) or export sequences (NESs), located within the cargo protein, with import receptor proteins (importins) or export receptor proteins (exportins), which mediate translocation of the cargo across the nuclear envelope (Jans et al., 2000; Pemberton and Paschal, 2005; Poon and Jans, 2005). To activate transcription, transcription factors must be within the nuclear compartment; thus, modulation of transcription factor nuclear import and/or export is a potent regulatory mechanism. Numerous mechanisms are reported to regulate nuclear transport of transcription factors and other nucleocytoplasmic proteins by affecting the interaction of importins and exportins with NLSs or NESs, respectively (Gardner and Montminy, 2005; Jans et al., 2000; Pemberton and Paschal, 2005; Poon and Jans, 2005). For example, the transcription factors signal transducers and activators of transcription (STATs) STAT1 and STAT2 exist in a latent monomeric state until activation by phosphorylation and dimerisation, accompanied by activation of NLS function, results in accumulation of STAT dimers in the nucleus (Randall and Goodbourn, 2008).

Recent data, however, indicate that nuclear import-export can be subject to regulation additional to simple signal recognition by importins or exportins. Specifically, components of the cytoskeleton, particularly the microtubule (MT) network, can affect nuclear trafficking of specific proteins (Campbell and Hope, 2003; Giannakakou et al., 2000; Lam et al., 2002; Mikenberg et al., 2007; Moseley et al., 2007b; Rathinasamy and Panda, 2008; Roth et al., 2007). Intriguingly, there exist two opposing modes of MT-regulated nuclear import. In the first (MT-facilitated import), the nuclear localisation of proteins such as p53, parathyroid hormone-related protein, retinoblastoma protein (Rb), and the rabies virus P-protein (RPP) can be facilitated by MTs (Campbell and Hope, 2003; Giannakakou et al., 2000; Lam et al., 2002; Mikenberg et al., 2007; Moseley et al., 2007b; Rathinasamy and Panda, 2008; Roth et al., 2007). This generally involves the MT motor dynein, which mediates movement on MTs from the cell periphery to the perinuclear region (Dohner et al., 2005), and therefore, MTs and dynein are thought to shuttle protein cargo toward the nucleus, resulting in enhanced nuclear import kinetics (Lam et al., 2002; Moseley et al., 2007b; Roth et al., 2007). In the second mode (MT-inhibited import), protein association with MTs, involving sequestration to the cytoplasm, results in inhibition of nuclear import (Campbell and Hope, 2003; Haller et al., 2004; Malki et al., 2005; Yamasaki et al., 2005; Ziegler and Ghosh, 2005).

Importantly, it has been shown that MT facilitation or MT inhibition of import is a property of a select group of nuclear-trafficking proteins and that conventional importin-mediated nuclear import of other proteins is independent of the MT cytoskeleton, including import of interferon (IFN)-activated STAT1 (Lillemeier

et al., 2001; Roth et al., 2007). Thus, MTs do not have an integral role in the nuclear import of all proteins, but interact directly or indirectly with certain proteins via specific sequences therein (MT-association sequences, MTASs) to affect subcellular localisation. This is supported by the fact that NLS-containing MT-facilitated-type proteins can revert to conventional MT-independent import as a result of deleting the MTAS, and that a particular form of MTASs (dynein light chain association sequences, DLCASs) found in a number of viral or cellular proteins including RPP, can confer a MT-facilitated phenotype on MT-independent NLS-containing proteins (Moseley et al., 2007b).

Nuclear trafficking of transcription factors is central to the innate immune response to viral infection, which is mediated by the IFN system (Chelbi-Alix et al., 2006; Haller et al., 2006; Randall and Goodbourn, 2008). Viral infection results in the activation of transcription factors such as NF-κB and IRF3, which translocate to the nucleus to activate IFN gene transcription (Randall and Goodbourn, 2008). The IFN gene products, such as IFNβ, act in an autocrine and paracrine fashion, binding to IFN receptors on the cell surface to initiate Jak-STAT-signalling pathways and activate STAT1 and STAT2 (see above). Nuclear-localised STAT transcription factor complexes then activate specific sequences [IFN-sensitive response elements (ISREs) for IFNα/β] in the promoter regions of IFN-sensitive genes, culminating in the expression of hundreds of IFN-responsive proteins that establish the cellular antiviral state (Chelbi-Alix et al., 2006; Haller et al., 2006; Randall and Goodbourn, 2008). Viral evasion of the IFN response is therefore an essential component of viral infection, and is achieved by the expression of virus-encoded proteins (IFN-antagonists), including the rabies virus protein RPP, which inhibit the IFN system via diverse mechanisms (Brzozka et al., 2005; Brzozka et al., 2006; Chelbi-Alix et al., 2006; Randall and Goodbourn, 2008; Shimizu et al., 2006; Vidy et al., 2005). The capacity of a virus to antagonise IFN is also a determinant of its ability to infect multiple species (Randall and Goodbourn, 2008), the significance of which is highlighted by recent outbreaks of emerging zoonotic viruses in human populations (e.g. SARS and Nipah virus) and the persistence of others, such as rabies virus (the cause of >50,000 human fatalities per year) and Ebola virus.

Here, we show for the first time that the P3 protein (a truncated version of RPP, produced by leaky scanning in rabies-virus-infected cells) (Fig. 1) (Chenik et al., 1995), forms MT-inhibited-type interactions with MTs. These interactions are dependent on the oligomeric state of RPP, suggesting that it may be able to switch dynamically between MT-inhibited and MT-facilitated modes. This represents the first evidence that a protein can undergo dual modes of MT association to regulate nuclear trafficking. We further show that P3 protein can cause the MT-independent-type protein STAT1 to form MT-inhibitory associations, resulting in sequestration of STAT1 away from the nucleus and inhibition of IFN signalling that is dependent on MTs and on the oligomeric state of RPP. This is the first report of MT function in viral IFN antagonism and identifies a novel mechanism to regulate STAT transcriptional activity, whereby the IFN-antagonist protein tethers STATs to the cytoskeleton, preventing signal transduction vital to the establishment of an antiviral state.

Results

The MT cytoskeleton can negatively regulate P3 nuclear localisation

We previously showed that the DLC-AS region within residues 139-172 of RPP is able to confer MT-facilitated nuclear import on MT-independent-type protein constructs containing the RPP NLS (residues 174-297) or heterologous NLSs (Moseley et al., 2007b). The main rabies-virus-expressed form of RPP able to localise to the nucleus is the P3 protein (residues 54-297); this is due to the absence of residues 1-53, which inactivates the strong NES (NES1) that causes nuclear exclusion of full-length RPP, P1 (residues 1-297) (Fig. 1).

To analyse the role of MTs in nuclear import of P3, we transfected Vero cells to express GFP-P3 or GFP-RPP$_{139-297}$ before treatment with or without the MT-disrupting drug nocodazole (NCZ) and analysis of subcellular localisation by quantitative confocal laser scanning microscopy (CLSM) (Fig. 2) to determine the ratio of nuclear to cytoplasmic fluorescence (Fn/c) (Moseley et al., 2007a; Moseley et al., 2007b; Roth et al., 2007). The results confirmed previous observations that GFP-RPP$_{139-297}$ uses a MT-facilitated import mechanism, as indicated by a reproducible and significant decrease in nuclear accumulation of GFP-RPP$_{139-297}$ in NCZ-treated cells compared with untreated cells (Fig. 2B) (Moseley et al., 2007b). Conversely, GFP-P3 showed a significant increase in nuclear localisation following NCZ treatment, which is indicative of a MT-inhibited mechanism (Fig. 2B). The nuclear import of MT-independent-type proteins such as GFP and GFP-fused NLSs (e.g.

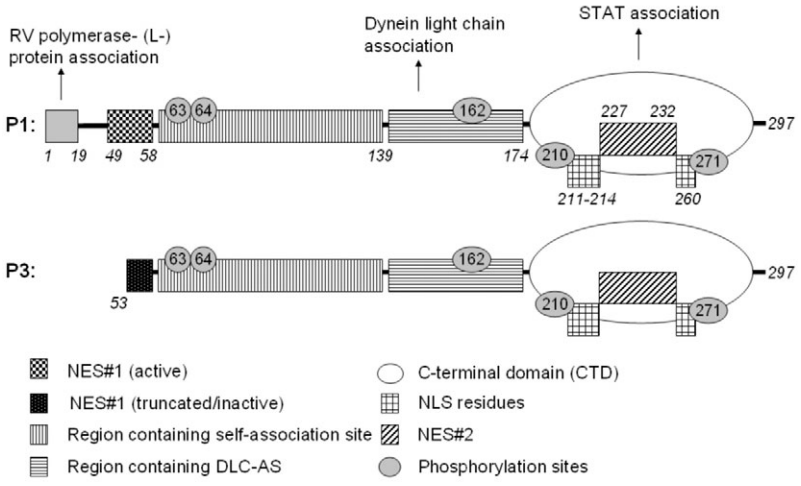

Fig. 1. Schematic diagram of RPP. Leaky scanning results in the expression of five proteins (Chenik et al., 1995) of which P1 and P3 are shown. The nuclear localisation of RPP has been shown to depend on the interplay of NES1, NES2, the NLS and DLC-AS (Moseley et al., 2007a; Moseley et al., 2007b; Pasdeloup et al., 2005). The molecular interactions of RPP modules are indicated, with the position of the modules in the protein sequence indicated by residue numbers in italics. Phosphorylation sites are also highlighted.

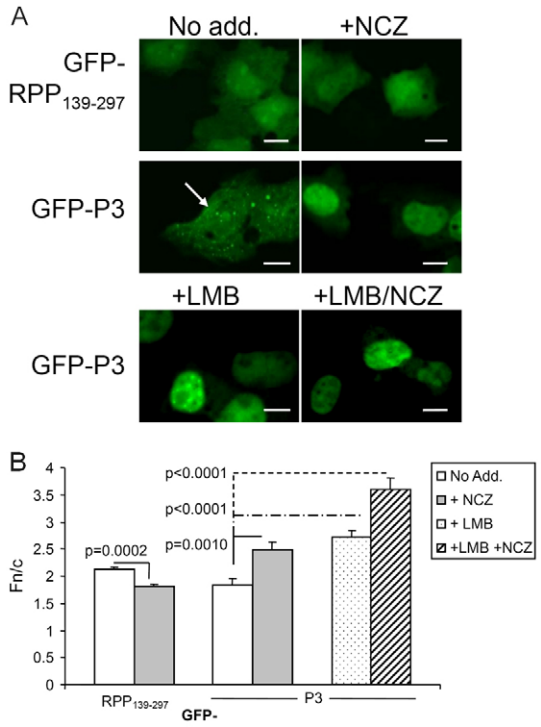

Fig. 2. The MT cytoskeleton negatively regulates P3 nuclear localisation. (A) Vero cells were transfected to express the indicated proteins and treated without or with NCZ and/or LMB (4 hours) before routine CLSM imaging focussed at the midpoint of the nucleus. The white arrow indicates interaction of GFP-P3 with cytoplasmic structures. Scale bars: 10 μm. (B) Images such as those shown were analysed to calculate the ratio of nuclear to cytoplasmic fluorescence (Fn/c) corrected for background. Results are mean ± s.e.m. of n>40 and are representative of three or more separate assays.

the SV40 large-T antigen NLS, ppUL44 human cytomegalovirus NLS) was unaffected by NCZ (data not shown) (see Moseley et al., 2007b). Thus, the MT-facilitated mechanism enhancing nuclear import of the short RPP fragment $RPP_{139-297}$ was switched to a MT-inhibited mechanism in P3.

Although NES1 is inactive in P3, it contains a second NES (NES2) in the C-terminal domain (CTD; residues 174-297) (Fig. 1) (Moseley et al., 2007a; Pasdeloup et al., 2005). We therefore examined the effect of the nuclear export inhibitor leptomycin B (LMB, which specifically affects transport mediated by the exportin CRM1) on MT-dependent nucleocytoplasmic localisation of P3. As previously reported, LMB treatment significantly increased nuclear localisation of GFP-P3 (Fig. 2B) (Moseley et al., 2007a). Significantly, this localisation was further increased by combined treatment with LMB and NCZ (Fig. 2B). Thus, it appears that P3 nuclear localisation is negatively regulated by the combined action of nuclear export and MT-inhibitory mechanisms.

GFP-P3 can stably associate with MTs, involving several RPP domains

Although the DLC-AS of RPP is able to confer a MT-facilitated phenotype on proteins (Moseley et al., 2007b), it does not appear to result in stable association with MTs in transfected cells, i.e. DLC-AS-containing proteins do not decorate MTs in a fashion detectable by CLSM (Moseley et al., 2007b), which is consistent with dynamic, transient association of the RPP-DLC-AS with MTs for MT-facilitated nuclear import. By contrast, a stable, MT-inhibited mode of interaction would be expected to be revealed by association with MTs when viewed by microscopy. Routine CLSM indicated that GFP-P3 does associate with cytoplasmic structures (Fig. 2A). To characterise these structures, we used high-resolution CLSM to analyse Vero cells transfected with GFP-P3 and detected a clear association with filamentous structures in the cytoplasm (Fig. 3A upper panel and not shown). We observed a similar association of transfected GFP-P3 with filamentous structures in HeLa, BSR, U-373-MG and Cos-7 cells (not shown). To examine the contribution of different domains of RPP to MT association, we expressed in Vero cells several forms of RPP fused to GFP: P1 (residues 1-297, which contains the functional NES1); $RPP_{139-297}$ (which contains the DLC-AS and the CTD); $RPP_{174-297}$ (the CTD alone, which contains the NLS and NES2); and the regions RPP_{1-172} and RPP_{54-172} (which contain the RPP self-association region, with or without, respectively, an intact NES1) (see Fig. 1). As can be seen in Fig. 3A (lower panel), and in contrast to GFP-P3, none of GFP-P1, GFP-$RPP_{139-297}$, GFP-$RPP_{174-297}$, GFP-RPP_{1-172} or GFP-RPP_{54-172} showed any detectable association with cytoplasmic filaments. Treatment of cells with the MT-stabilising drug taxol (TAX) resulted in a more extensive interaction of GFP-P3 with filaments, indicating that the structures represent MTs, but no cytoplasmic filament association of the other proteins was detected (Fig. 3A). Thus, it appears that none of the modules tested are sufficient alone to mediate stable MT-association of GFP, and that this mode of association requires several domains within P3. Intriguingly, it also appears that although the sequences required for stable MT association are found within P3 (residues 54-297), this property is inhibited by the presence of the additional residues 1-53 in P1.

As expected, GFP-P1 and RPP_{1-172}, which contain the functional NES1, were excluded from the nucleus, whereas GFP-P3, GFP-$RPP_{139-297}$, GFP-$RPP_{174-297}$, and GFP-RPP_{54-172} were distributed between the nucleus and cytoplasm to different extents (Moseley et al., 2007a; Pasdeloup et al., 2005). Interestingly, although GFP-$RPP_{174-297}$ and GFP-$RPP_{139-297}$ showed moderate nuclear accumulation (Fn/c for GFP-$RPP_{139-297}$ of 2.12±0.05; mean ± s.e.m. for n>40) (Fig. 2B, Fig. 3A), GFP-RPP_{54-172} accumulated to a much greater extent (Fn/c= 3.4±0.12; Fig. 3A and not shown), to a level comparable with that of GFP-P3 in the presence of LMB and NCZ (Fn/c=3.59±0.21; Fig. 2B). Thus, RPP_{54-172} appears to possess nuclear-localising activity that might contribute to P3 nuclear accumulation.

To confirm that the filaments observed in P3-transfected cells were indeed MTs, we treated GFP-P3-expressing cells with or without TAX or NCZ before fixation and immunostaining for the MT component β-tubulin. This revealed a clear colocalisation of filamentous GFP-P3 with tubulin in the form of MTs, confirming that GFP-P3 associates with the MT cytoskeleton (Fig. 3B and supplementary material Fig. S1A). Treatment of cells with TAX resulted in more extensive association or bundling of the GFP-P3-MT structures whereas NCZ treatment clearly disassembled the structures, resulting in a diffuse appearance of GFP-P3 and tubulin (Fig. 3B). We also confirmed that P3 was associated with MTs in intact, live cells by transfecting cells to coexpress GFP-P3 with α-tubulin fused to mCherry (tubulin-mCherry) (Shaner et al., 2004) or mCherry-P3 with α-tubulin fused to GFP (tubulin-GFP), finding that filamentous P3 clearly colocalises with α-tubulin-containing filaments (supplementary material Fig. S1B,C).

To confirm the physical association of GFP-P3 with MTs, we purified MTs and MT-associated proteins from cell lysates as

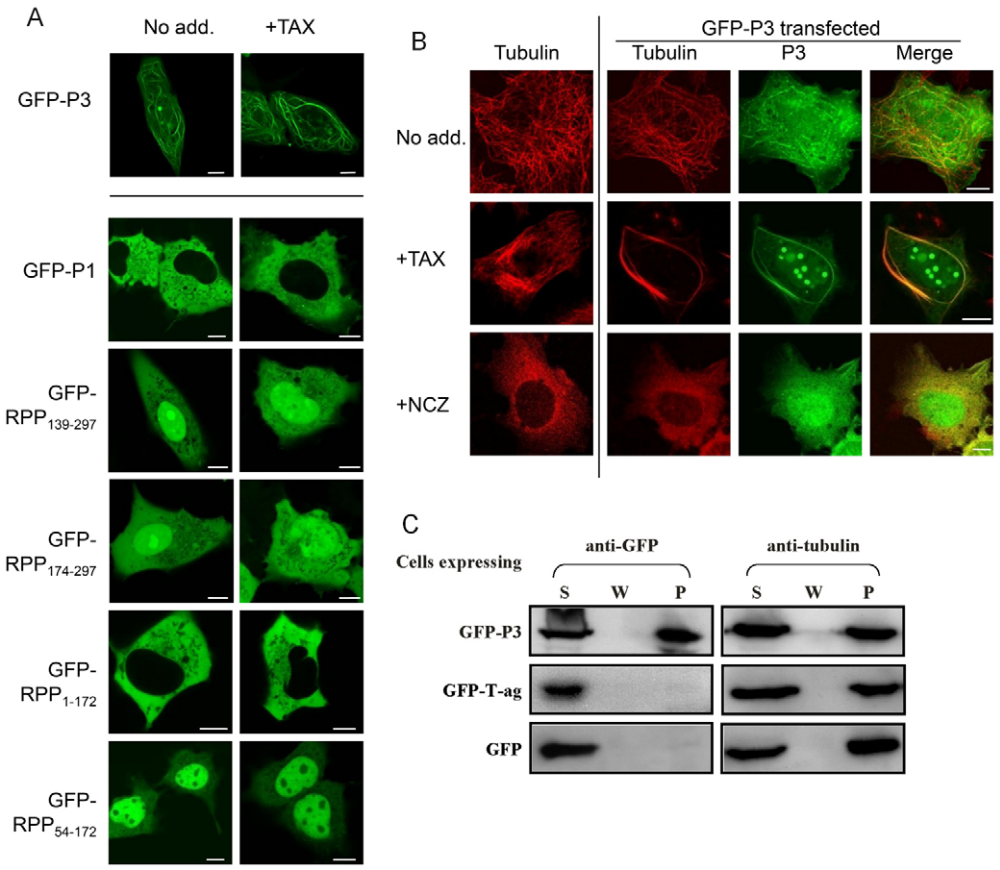

Fig. 3. P3 protein interacts specifically with MTs by a mechanism requiring several RPP domains. Vero cells were transfected with the indicated constructs and imaged by high-resolution CLSM, following treatment without or with MT-stabilising (+TAX) or MT-disrupting (+NCZ) drugs. (A) CLSM of live cells revealed the association of GFP-fused protein with filamentous structures in the cytoplasm of cells expressing GFP-P3 (upper panel) but not other GFP-fused RPP derivatives (lower panel); the results were reproduced in three or more separate assays in Vero and 1 or more assays in Cos7 and HeLa cells. (B) Vero cells expressing GFP-P3 and treated as indicated were fixed with paraformaldehyde and immunostained for tubulin (red) before analysis by CLSM. Colocalisation is apparent as yellow coloration in the merged panels. Similar results were obtained in three or more separate assays in Vero cells and one or more assays in Cos7 cells. Scale bars: 10 μm. (C) Cos-7 cells transfected with GFP-P3, GFP-T-ag NLS or GFP alone were lysed in MT-stabilising buffer and submitted to ultracentrifugation to separate the supernatant (S, containing soluble tubulin), wash (W) and pellet (P, containing MTs and MT-associated proteins). Fractions were then subjected to western analysis using anti-GFP or anti-β-tubulin.

previously described (Roth et al., 2007). Cells were transfected to express GFP-P3 or, as negative controls, GFP or GFP fused to the NLS from SV40 large-T antigen (GFP-T-ag), neither of which associate with MTs (Roth et al., 2007). As shown in Fig. 3C, GFP-P3, GFP alone and GFP-T-ag were present in the soluble (S) fraction, but only P3 was present in the MT fraction (pellet, P). Thus, the biochemical data (Fig. 3C) indicate that P3 can physically associate with MTs isolated from lysed cells, and this supports the key observations from CLSM that GFP-P3 associates with MTs in the context of live, intact cells (Fig. 3A,B and supplementary material Fig. S1).

Association of P3 with MTs is dependent on dimerisation

In vitro, RPP exists in an equilibrium between monomeric and oligomeric forms (Gigant et al., 2000). Since RPP_{54-139} contains the RPP self-association domain (Mavrakis et al., 2004), $RPP_{139-297}$ would be predicted to exist as a monomer, whereas P3, which can interact stably with MTs (see above), can exist in both monomeric and oligomeric states. Thus, interaction of RPP with MTs might depend strongly on oligomerisation. To test this possibility, we replaced the region 54-139 of P3 with a heterologous dimerisation module, using the Ariad inducible homodimerisation kit (see Materials and Methods). The module, Fv1, is a variant of the FKBP protein that can be induced to dimerise by the addition of a cell-permeable dimerisation reagent (DR), AP20187. To monitor the subcellular localisation of Fv1-containing protein, the Fv1 was fused in-frame C-terminal to GFP in pEGFP-C1 with RPP fragments subsequently cloned in-frame C-terminal to the GFP-Fv1 open reading frame. As shown in Fig. 4A, no filamentous structures were detected in cells expressing GFP-Fv1 alone or GFP-Fv1 fused to various forms of RPP. However, following addition of DR to cells, a clear association of GFP-fusion protein with MTs was detected in cells expressing GFP-Fv1-$RPP_{139-297}$, which became obvious following TAX treatment, indicating that $RPP_{139-297}$ contains the MTAS sequence and is necessary and sufficient to mediate stable RPP-MT association, dependent on dimerisation. The specificity of this effect was demonstrated by the fact that neither GFP-Fv1 nor GFP-$RPP_{139-297}$ could be induced to associate with filamentous structures following treatment with DR with or without TAX (Fig. 4A). Treatment with TAX alone did not induce association of Fv1-containing GFP-fusion proteins with MTs (see supplementary material Fig. S2A).

We were also able to detect some MT association of GFP-Fv1-$RPP_{174-297}$ in DR-treated cells, which was more obvious in cells treated with both DR and TAX, but in both cases, MT association was considerably reduced compared with that observed for GFP-Fv1-$RPP_{139-297}$ in equivalently treated cells (Fig. 4A). This indicated that efficient dimerisation-dependent MT association of the region $RPP_{139-297}$ requires both the DLC-AS ($RPP_{139-172}$) and CTD ($RPP_{174-297}$). However, no clear association of DR-dimerised GFP-Fv1-$RPP_{139-172}$ with MTs was observed in cells treated with or without TAX (Fig. 4A). Thus $RPP_{139-172}$ is not sufficient to mediate MT association, but facilitates MT association conferred by $RPP_{174-297}$. To confirm that the filamentous structures with which dimerised GFP-Fv1-$RPP_{174-297}$ and GFP-Fv1-$RPP_{139-297}$ associate are MTs, transfected cells treated with DR and/or TAX were fixed and immunostained for tubulin revealing that the filament-associated GFP-fused proteins in cells treated with DR or DR and TAX were colocalised with MTs (Figs 4B and supplementary material Fig. S2B), whereas no filamentous MT association of GFP-Fv1-$RPP_{174-297}$ and GFP-Fv1-$RPP_{139-297}$ was observed in untreated cells or cells treated with TAX alone (supplementary material Fig. S2B).

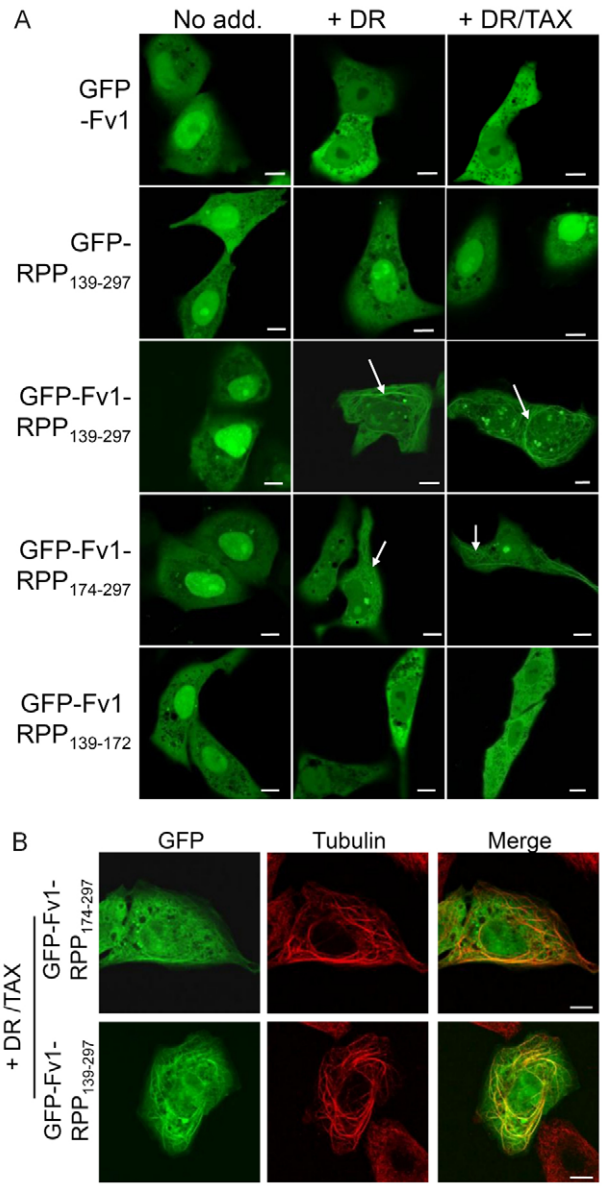

Fig. 4. Stable MT association of RPP is dependent on dimerisation of the C-terminal region. (A) Vero cells were transfected with the indicated constructs and treated with or without DR (2 hours) and/or TAX (4 hours) before analysis of live cells by high-resolution CLSM. MT association of GFP was not detected in untreated cells but became apparent following DR treatment of cells expressing GFP-Fv1-$RPP_{139-297}$ or GFP-Fv1-$RPP_{174-297}$ (white arrows) and this became more obvious following treatment with TAX. No GFP-MT association was observed in cells expressing the other GFP-fused proteins tested. Treatment of cells with TAX alone did not cause association of any of the GFP-fusion proteins with MTs (see supplementary material Fig. S1A). Similar results were observed in three or more separate assays. (B) Vero cells transfected with GFP-Fv1-$RPP_{139-297}$ and GFP-Fv1-$RPP_{174-297}$ (green) were treated with DR and TAX before fixation and immunostaining for tubulin (red), and imaging by high-resolution CLSM. Similar results were observed in two or more separate assays. Scale bars: 10 μm.

Stable MT-association of P3 is independent of the dynein light chain LC8 and dynactin

Previously, we showed that MT facilitation of nuclear import of $RPP_{139-297}$ is dependent on the DLC-AS (within residues 139-172), and can be inhibited by mutation (D_{143}/Q_{147}-A) to prevent association with the dynein light chain LC8 (Moseley et al., 2007b; Poisson et al., 2001; Raux et al., 2000). Thus, in common with other MT-facilitated proteins (e.g. Rb and p53) (Giannakakou et al., 2000; Roth et al., 2007), MT-facilitated-nuclear import of $RPP_{139-297}$ appears to involve dynein components. MT-inhibitory-type interactions of proteins, however, do not appear to depend on dynein.

We therefore examined the MT association of P3 and dimerised $RPP_{139-297}$ harbouring the D_{143}/Q_{147}-A mutation by transfection and CLSM analysis. Both P3(D_{143}/Q_{147}-A) and dimerised Fv1-$RPP_{139-297}$(D_{143}/Q_{147}-A) retained the capacity to decorate the cytoplasmic MT filaments of transfected cells (Fig. 5A), implying that stable MT association of these proteins is independent of LC8 association via the DLC-AS. As expected, Fv1-$RPP_{139-297}$(D_{143}/Q_{147}-A) does not associate with filamentous structures in cells not treated with DR (supplementary material Fig. S3A).

Cargo interactions with dynein and MTs frequently involve the dynein-associated dynactin complex (Dohner et al., 2005). The complex can be disassembled by overexpression of the dynactin component dynamitin, which is used as a standard method to examine dependency of processes, including MT-facilitated nuclear import, on dynein and dynactin function (Giannakakou et al., 2000; Roth et al., 2007). We therefore tested the capacity of P3 and dimerised $RPP_{139-297}$ to associate stably with MTs in cells overexpressing dynamitin fused to the monomeric fluorescent mCherry protein, which has previously been used to confirm the role of dynein and dynactin in nuclear import of p53 and Rb (Roth et al., 2007). As shown in Fig. 5B, overexpression of dynamitin-mCherry did not prevent stable MT association of GFP-P3 or dimerised GFP-Fv1-$RPP_{139-297}$. In cells expressing dynamitin-mCherry that were not treated with DR, GFP-Fv1-$RPP_{139-297}$ showed no association with filaments, as expected (supplementary material Fig. S3B). As a positive control for dynamitin overexpression, we confirmed our previous observations (Roth et al., 2007) that the nuclear localisation of the MT-facilitated-type protein GFP-Rb is significantly reduced in cells coexpressing dynamitin-mCherry compared with cells not expressing dynamitin-mCherry. Expression of dynamitin-mCherry significantly ($P>0.0006$) reduced nuclear localisation of GFP-Rb (Fn/c=12.9±3.2 and 23.8±2.9, $n>38$ for GFP-Rb in cells expressing or not expressing

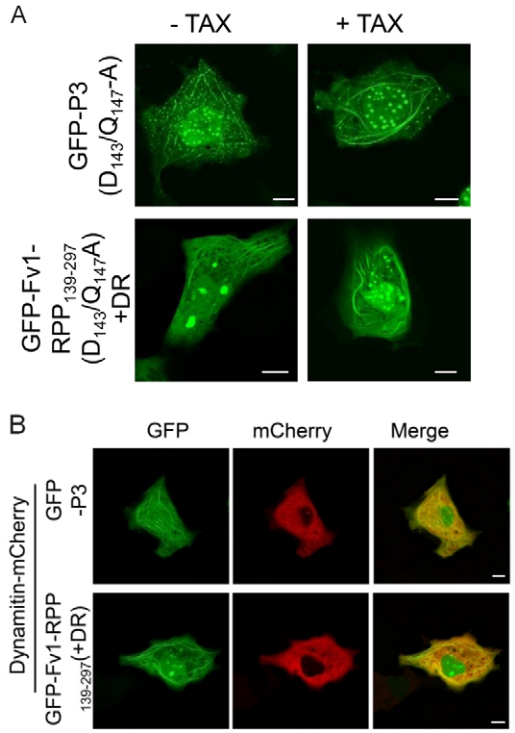

Fig. 5. Association with dynein light chain LC8 or dynactin is not required for P3-MT association. Cells were transfected with the indicated constructs and imaged live by high-resolution CLSM. (A) In Vero cells expressing GFP-P3(D_{143}/Q_{147}-A) or DR-treated cells expressing GFP-Fv1-$RPP_{139-297}$(D_{143}/Q_{147}-A), the GFP-fused protein can associate with MT-like filaments following treatment with or without TAX, similarly to the wild-type proteins (see Fig. 3A and Fig. 4A). These results were reproduced in two or more separate assays in Vero and Cos7 cells. (B) In Vero cells expressing GFP-P3 and in DR-treated cells expressing GFP-Fv1-$RPP_{139-297}$, MT-filament association of the GFP protein was evident in the presence of overexpressed dynamitin (dynamitin-mCherry). Scale bars: 10 μm.

dynamitin-mCherry, respectively). Thus, it appears that stable P3-MT association does not involve the commonly used dynein-dynactin complex and, in contrast to the MT-facilitated-type interaction of $RPP_{139-297}$, is not dependent on association with dynein LC8 so that the MT-facilitated and MT-inhibited modes of RPP-MT interaction appear to be physically distinct.

MT-P3 interaction causes MT association of STAT1

RPP is multifunctional, with roles as the rabies virus polymerase (L-protein) cofactor and as the IFN antagonist (Brzozka et al., 2005; Brzozka et al., 2006; Chelbi-Alix et al., 2006; Randall and Goodbourn, 2008; Shimizu et al., 2006; Vidy et al., 2005). P3 appears to be specialised for rabies-virus-mediated IFN antagonism, because it lacks the N-terminal interaction site for the L-protein (Chelbi-Alix et al., 2006) (Fig. 1), and is implicated in rabies virus effects both on STAT signalling and on the IFN-induced promyelocytic leukaemia nuclear bodies (PML-NBs) (Blondel et al., 2002; Chelbi-Alix et al., 2006; Vidy et al., 2007). RPP has been reported to interact with STATs and to inhibit their nuclear localisation (Brzozka et al., 2006; Vidy et al., 2005), but the mechanisms underlying this are not fully understood. We hypothesised that P3, via its stable interaction with MTs, might be able to draw STAT1 to the MT network causing its sequestration in the cytoplasm and thereby effecting an MT-inhibitory-type mechanism. We therefore examined whether P3 and STAT1 form complexes at MTs. As can be seen in Fig. 6A (upper panel), STAT1-dsRed showed a diffuse localisation in Vero cells, consistent with the known distribution of non-activated STAT1. We observed no localisation of STAT1 with cytoskeletal filaments, even if the MTs were stabilised by TAX treatment (Fig. 6A, upper panel). However, when coexpressed with GFP-P3, STAT1-dsRed became associated with MT-like filaments, where it colocalised with GFP-P3. The filaments were rendered more easily detectable following TAX treatment and were completely disrupted following NCZ treatment (Fig. 6A, lower panel).

We next tested the capacity of $RPP_{139-297}$ to cause association of STAT1 with MTs, dependent on dimerisation. As can be seen in Fig. 6B and supplementary material Fig. S3C, no localisation of GFP or dsRed with MTs was observed in cells expressing non-dimerised GFP-Fv1-$RPP_{139-297}$ with or without treatment with TAX or NCZ. However, following treatment with DR, both proteins were observed to associate with MT-like structures, which were eliminated by NCZ treatment and enhanced by TAX treatment (Fig. 6B). Thus, the association of P3 with MTs appears to be able to cause translocation of STAT1 from a diffuse localisation in the cytosol to become strongly associated with MTs.

P3 expression inhibits STAT1 nuclear import in IFN-activated cells by a MT-inhibitory-type mechanism

The capacity of P3 to cause stable association of STAT1 with MTs indicated that P3 might use a novel MT-dependent mechanism to inhibit nuclear import of STAT1 and thereby disable the innate immune response; i.e. P3 might be able to switch STAT1 nuclear import from a MT-independent to a MT-inhibited-type mechanism. We therefore examined quantitatively the nuclear accumulation of STAT1-dsRed in cells expressing or not expressing GFP-P3, with or without treatment with IFNα or IFNγ and with or without a disrupted MT network (Fig. 7A,B).

Quantitative analysis confirmed that, in the absence of GFP-P3 expression, STAT1-dsRed was diffusely distributed in Vero cells (Fig. 7A,B; Fn/c ~1.5). This was unaffected by NCZ treatment, indicating that the distribution of latent STAT1 does not involve any significant MT-dependent component (Fig. 7A,B). Treatment of cells with IFNα (Fig. 7A,B) or IFNγ (not shown) resulted in a significant translocation of STAT1-dsRed to the nucleus (Fig. 7A,B; Fn/c ~5.5 for IFNα), which was unaffected by NCZ treatment (Fig. 7B), indicating a MT-independent mechanism of IFN-induced STAT1 nuclear import, which is consistent with previous findings (Lillemeier et al., 2001). In the absence of P3 expression, the cytoplasmic fraction of STAT1-dsRed showed no association with cytoplasmic filaments whether cells were treated or not with IFN (Fig. 7A).

Coexpression of GFP-P3 with STAT1-dsRed resulted in nuclear exclusion of STAT1 (Fig. 7A,B; Fn/c ~0.5) with no significant increase in nuclear accumulation upon treatment with NCZ or IFN alone (Fig. 7B). Thus, in cells expressing P3, MT association is not solely responsible for the nuclear exclusion of STAT1-dsRed, and treatment with IFNα (Fig. 7A,B) or IFNγ (not shown) alone is not sufficient to effect nuclear accumulation of STAT1-dsRed. However, when cells were treated with both IFNα and NCZ (Fig. 7A,B) or IFNγ and NCZ (not shown), a significant enhancement of nuclear accumulation was observed (Fig. 7A,B; Fn/c ~1.5 for IFNα) within 2 hours of IFN treatment, which is consistent with a significant relocalisation of STAT1-dsRed protein to the nucleus in IFN-activated cells in the absence of an intact MT network. Expression of GFP without the P3 fusion partner did not block nuclear

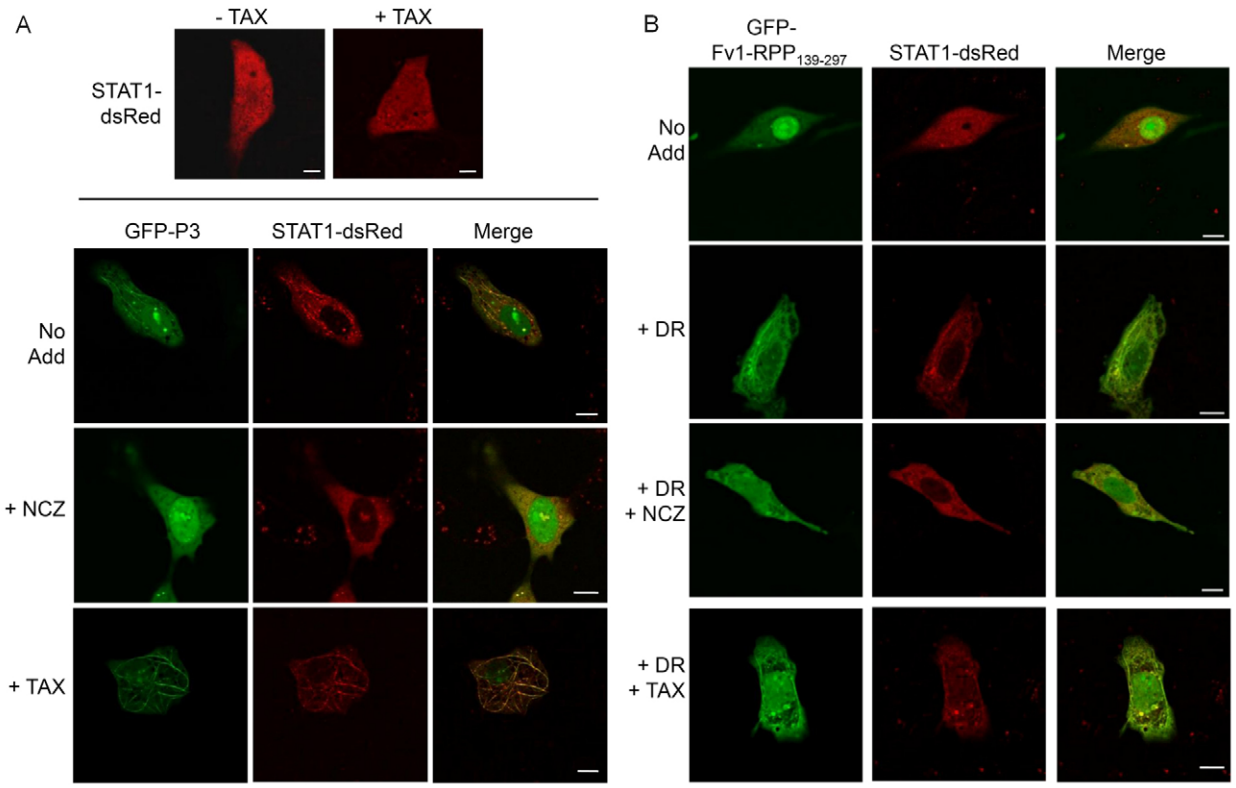

Fig. 6. P3 expression causes STAT1 to associate with MTs. Vero cells were transfected to express the indicated proteins before treatment with or without the indicated drug(s) and imaging live by high-resolution CLSM. (A) STAT1-dsRed expressed alone shows a diffuse localisation in the nucleus and cytoplasm (upper panel). Coexpression of GFP-P3 with STAT1-dsRed results in nuclear exclusion of STAT1-dsRed and colocalisation with GFP-P3 at cytoplasmic filaments, which are more obvious after TAX treatment (lower panel). NCZ treatment results in diffuse cytoplasmic appearance of GFP-P3 and STAT1-dsRed (lower panel). These data were reproduced in three or more separate assays. (B) Coexpression of GFP-Fv1-$RPP_{139-297}$ with STAT1-dsRed results in diffuse localisation of both proteins in the cytoplasm. Treatment with DR causes relocalisation of both proteins to associate with MTs, which is eliminated by NCZ treatment and made more obvious by TAX treatment. The data were reproduced in three or more separate assays. Scale bars: 10 μm.

accumulation of STAT1-dsRed (data not shown). Thus, P3 expression inhibited IFN-activated nuclear accumulation of STAT1-dsRed and this effect was dependent on MTs.

We also examined the effect of IFN and NCZ on the subcellular localisation of endogenous STAT1 in cells expressing or not expressing GFP-P3. Vero cells were transfected and treated as above before fixation and immunostaining using anti-STAT1 for CLSM and image analysis (Fig. 7C,D). Nuclear localisation of endogenous STAT1 in nontransfected cells was significantly increased in IFN-activated cells and was unaffected by NCZ (Fig. 7C,D). This is consistent with the observations made for STAT1-dsRed and confirmed that IFN-dependent STAT1 nuclear accumulation is MT independent.

In contrast to STAT1-dsRed in live intact cells, the nuclear localisation of endogenous STAT1 in fixed untreated cells was not significantly affected by GFP-P3 expression (Fig. 7C,D). This is probably due to the fact that STAT1 is overexpressed in the case of STAT1-dsRed. However, IFN-induced nuclear accumulation of endogenous STAT1 was inhibited in cells expressing GFP-P3, unless the cells were treated with NCZ (Fig. 7C,D); this is consistent with the effects observed for STAT1-dsRed expressed in live cells. Thus, it appears that GFP-P3 can switch endogenous STAT1 and STAT1-dsRed from MT-independent to MT-inhibited nuclear import as a mechanism to inhibit STAT1 nuclear accumulation in response to IFN.

Following IFNα binding to the IFN receptor, STAT1 becomes phosphorylated at Y701 by JAK1 tyrosine kinase, which precedes STAT1 accumulation in the nucleus (Randall and Goodbourn, 2008). Thus, the above data indicate that GFP-P3 impacts on the nuclear localisation of phosphorylated STAT1. To confirm this effect we examined the nuclear localisation of Y701-phosphorylated STAT1 (STAT1-*P*) specifically by immunostaining fixed cells with a STAT1-*P*-specific antibody and analysing its nuclear localisation. In cells not expressing GFP-P3, STAT1-*P* nuclear localisation was independent of MT disruption by NCZ (supplementary material Fig. S4), but in GFP-P3-positive cells, nuclear localisation of STAT1-*P* was significantly enhanced by MT disruption, indicating that STAT1-*P* nuclear import is inhibited by P3, with dependence on MTs. This is consistent with results observed for total endogenous STAT1 or transfected STAT1-dsRed.

P3 expression or rabies virus infection inhibits IFN signalling and this effect is dependent on MTs

To establish the functional impact of the MT-dependent effect of P3 on STAT1 nuclear import, we examined the capacity of IFNα to stimulate STAT1-dependent activation of transcription using a luciferase reporter gene assay with luciferase expression under the control of an ISRE promoter (Vidy et al., 2005; Vidy et al., 2007). Cells were transfected with pISREluc and pRL-TK with or without cotransfection with GFP-P3 or GFP lacking a fusion partner, and

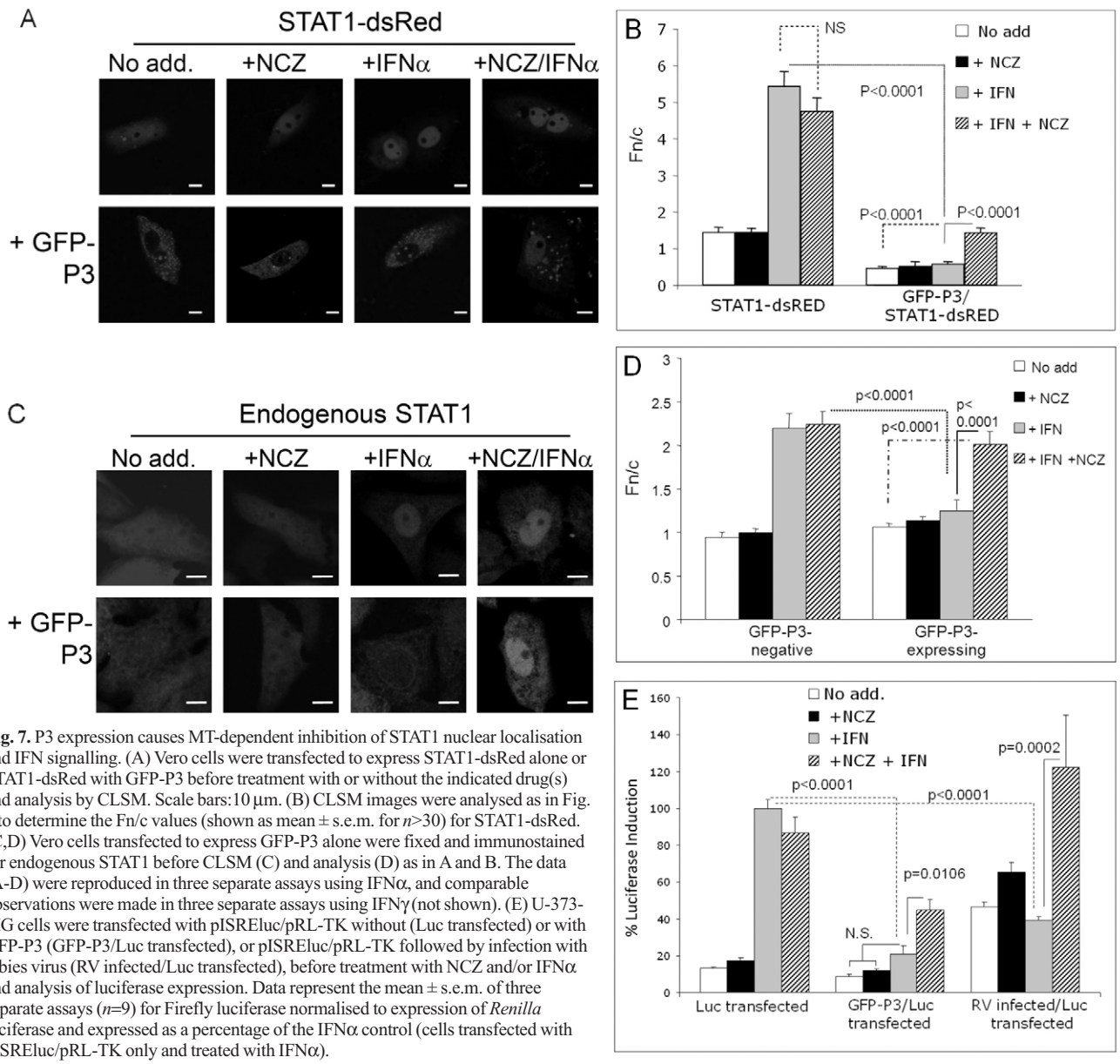

Fig. 7. P3 expression causes MT-dependent inhibition of STAT1 nuclear localisation and IFN signalling. (A) Vero cells were transfected to express STAT1-dsRed alone or STAT1-dsRed with GFP-P3 before treatment with or without the indicated drug(s) and analysis by CLSM. Scale bars:10 µm. (B) CLSM images were analysed as in Fig. 2 to determine the Fn/c values (shown as mean ± s.e.m. for n>30) for STAT1-dsRed. (C,D) Vero cells transfected to express GFP-P3 alone were fixed and immunostained for endogenous STAT1 before CLSM (C) and analysis (D) as in A and B. The data (A-D) were reproduced in three separate assays using IFNα, and comparable observations were made in three separate assays using IFNγ (not shown). (E) U-373-MG cells were transfected with pISREluc/pRL-TK without (Luc transfected) or with GFP-P3 (GFP-P3/Luc transfected), or pISREluc/pRL-TK followed by infection with rabies virus (RV infected/Luc transfected), before treatment with NCZ and/or IFNα and analysis of luciferase expression. Data represent the mean ± s.e.m. of three separate assays (n=9) for Firefly luciferase normalised to expression of *Renilla* luciferase and expressed as a percentage of the IFNα control (cells transfected with pISREluc/pRL-TK only and treated with IFNα).

the expression of luciferase was assessed following IFNα treatment of cells with or without NCZ pretreatment.

In cells expressing pISREluc and pRL-TK only, IFNα treatment significantly induced expression of luciferase compared with untreated cells (~tenfold increase, Fig. 7E). As expected from the lack of an effect of NCZ on STAT1 nuclear localisation (Fig. 7A-D), NCZ treatment did not significantly affect expression of luciferase in cells treated without or with IFNα (Fig. 7E). Identical results were obtained in cells cotransfected with pIRESluc, pRL-TK and GFP (data not shown).

In GFP-P3-expressing cells, we observed a significant reduction (to about 20%) in luciferase induction in response to IFNα treatment compared with cells not expressing GFP-P3 (Fig. 7E). In contrast to cells transfected with pISREluc and pRL-TK vector only, NCZ treatment of cells cotransfected with GFP-P3 produced a significant increase (>twofold) in induction of luciferase by IFNα, which is consistent with a substantial role for a MT-inhibitory-type mechanism in P3-mediated negative regulation of IFNα signalling.

To examine this effect in the context of rabies virus infection, we infected pISREluc/pRL-TK transfected cells with CVS strain rabies virus and tested the responsiveness to IFNα, with or without NCZ treatment, as above. As can be seen in Fig. 7E, IFNα-stimulated luciferase expression was significantly reduced (to about 40%) in infected cells compared with uninfected cells. In similar fashion to GFP-P3-transfected cells, this decrease was dependent on the MT network, because NCZ treatment significantly enhanced (~threefold) luciferase expression.

As our data implicated dimerisation in MT association of P3 and P3-associated STAT1 (see above), we next tested the effect of dimerisation of RPP on IFN-induced transcriptional activation. Cells were transfected with pISREluc/pRL-TK and vectors for expression of GFP-Fv1-$RPP_{139-297}$ or GFP-Fv1, before treatment with DR

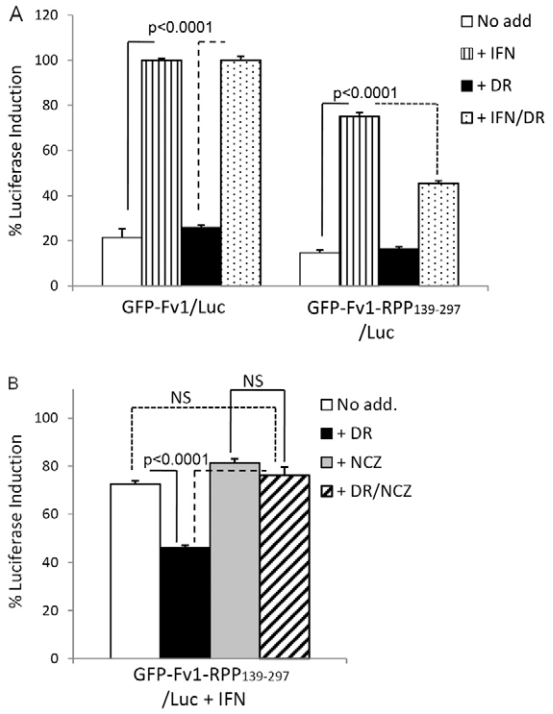

Fig. 8. Dimerisation-dependent inhibition of IFN signaling by $RPP_{139-297}$ is dependent on MTs. (A) U-373-MG cells were transfected with pISREluc/pRL-TK and GFP-Fv1-$RPP_{139-297}$ (GFP-Fv1-$RPP_{139-297}$/Luc) or GFP-Fv1 (GFP-Fv1/Luc), before treatment with DR and/or IFNα and analysis of luciferase expression. (B) GFP-Fv1-$RPP_{139-297}$/Luc transfected cells were treated with DR and/or NCZ before IFNα treatment, and analysis of luciferase expression. Data represent the mean ± s.e.m. of two or more separate assays ($n \geq 6$) for Firefly luciferase normalised to expression of *Renilla* luciferase and expressed as a percentage of the IFNα control (cells transfected with pISREluc/pRL-TK/GFP-Fv1 and treated with IFNα).

and/or NCZ followed by IFNα treatment. IFN treatment of cells expressing the luciferase vectors and GFP-Fv1 or GFP-Fv1-$RPP_{139-297}$ resulted in a significant increase in luciferase expression (Fig. 8A). The level of induction of luciferase in GFP-Fv1-transfected cells was equivalent to that in cells expressing pISREluc/pRL-TK only (not shown) confirming that GFP-Fv1 did not affect IFN-dependent signalling. DR treatment had no effect on IFN induction of luciferase expression in cells transfected with pISREluc/pRL-TK vectors only (not shown) or cotransfected with GFP-Fv1 (Fig. 8A), but caused a significant inhibition of luciferase induction in cells expressing GFP-Fv1-$RPP_{139-297}$, implying that dimerisation of the C-terminal region of RPP activates an IFN-antagonist mechanism.

To examine the role of MTs in this dimerisation-dependent mechanism, we treated pISREluc/pRL-TK/GFP-Fv1-$RPP_{139-297}$-transfected cells with DR and/or NCZ before addition of IFNα. Treatment of DR-treated cells with NCZ entirely negated the inhibitory effect of DR on luciferase induction, such that IFN-induced luciferase expression in cells treated with DR and NCZ was not different to that in untreated cells or cells treated with NCZ alone (Fig. 8B). This indicates that the dimerisation-dependent inhibition of IFN signalling by RPP is dependent on the integrity of the MT cytoskeleton.

Thus, STAT1 nuclear import and associated transcriptional activation of ISRE-dependent genes would appear to be independent of MTs unless the cells coexpress P3 protein. In the latter case, STAT1 appears to become tethered to MTs by P3, switching STAT1 nuclear import from a MT-independent to a MT-inhibited-type mechanism, with concomitant effects on cellular IFN signalling. The results strongly support the hypothesis that this mechanism is a crucial component in viral antagonism of IFN signalling.

Discussion

This study establishes a role for MTs in viral antagonism of IFN responses for the first time. Specifically, we have shown that the rabies virus IFN antagonist P3 is able to cause interaction of STAT1 with MTs in order to prevent STAT1 nuclear import, thereby disabling the IFN-signalling pathway that is vital to the innate antiviral immune response.

The mechanisms evolved by viruses to evade the innate immune response are extraordinarily varied, with IFN antagonists frequently able to perform a myriad of functions, both in the basic viral life cycle and in evasion of the antiviral response (Randall and Goodbourn, 2008). This might be particularly true of viruses with limited coding capacity such as rabies virus, which, in common with a number of other RNA viruses [e.g. Nipah, measles and Sendai (Randall and Goodbourn, 2008; Shaw et al., 2004)], uses products of the P gene for IFN-antagonist functions. RPP displays many archetypal features of IFN antagonists: it is multifunctional (with housekeeping roles in viral replication as well as roles in IFN antagonism) (Chelbi-Alix et al., 2006; Randall and Goodbourn, 2008) and expressed in several forms (see Fig. 1) (Chenik et al., 1995; Pasdeloup et al., 2005). Significantly, owing to the presence or absence of NESs and NLSs, the different gene products are able to accumulate differentially in the nucleus and the cytoplasm (Moseley et al., 2007a; Pasdeloup et al., 2005) and can thereby affect IFN signalling at several stages by affecting the functions of signalling and effector proteins of the IFN system located in different compartments. Specifically, RPP has been reported to inhibit phosphorylation of cytoplasmic IRF3, to interact with nuclear and cytoplasmic STAT1, which affects subcellular localisation and DNA binding, and to affect nuclear PML-NBs (Blondel et al., 2002; Brzozka et al., 2005; Brzozka et al., 2006; Chelbi-Alix et al., 2006; Vidy et al., 2005; Vidy et al., 2007). Thus, RPP counters the IFN system by the combined action of several distinct mechanisms. Consistent with this, our data (Fig. 7E) indicate that IFN antagonism by P3 involves a significant MT-dependent component, as well as contribution by other mechanism(s) that are not disabled by MT disruption, to produce full inhibition of IFN signalling. Interestingly, our data also indicate that MT-dependent IFN antagonism by RPP is dependent on its oligomeric state, which correlates with a role for oligomerisation in regulating RPP-MT association (see below), and indicates that the mechanisms of IFN antagonism mediated by RPP may be dynamically regulated.

It is intriguing that although RNA viruses such as rabies virus ostensibly have no need to interact with the nucleus, nuclear trafficking has been reported as a feature of numerous RNA-virus-encoded proteins, including known IFN antagonists (e.g. Billecocq et al., 2004; Breakwell et al., 2007; Chelbi-Alix et al., 2006; Ghildyal et al., 2009; Montgomery and Johnston, 2007; Nishie et al., 2007; Rawlinson et al., 2009; Shaw et al., 2005; Shaw et al., 2004) and the capacity of viruses to regulate nuclear import and/or export functions of cellular proteins is a key mechanism in IFN antagonism (Randall and Goodbourn, 2008). The latter includes various strategies to prevent STAT nuclear accumulation and activation of transcription, including STAT degradation, inhibition of

dimerisation, alteration or inhibition of phosphorylation, and sequestration into high molecular weight complexes (Randall and Goodbourn, 2008). The demonstration in the present report that IFN antagonists can exploit cellular MT cytoskeleton-dependent mechanisms to inhibit STAT1 nuclear accumulation highlights the diversity and intricacy of viral strategies to surmount the innate immune response. Given the potency of this mechanism to prevent IFN-dependent signalling (Fig. 7E), it seems likely that similar strategies will be used by other viruses, and might be implicated in previously reported cases of IFN-antagonist-mediated inhibition of STAT1 signalling.

In this report, we have also demonstrated the importance of dimerisation in MT association of RPP. It has been reported that certain cellular proteins associate with MTs as dimers (Short et al., 2002), indicating that oligomerisation might be involved in MTAS function. That stable MT association of RPP is dependent on oligomerisation is indicated by the fact that it is prevented by deletion of the endogenous self-association region of RPP (producing the truncated form, $RPP_{139-297}$), but can be reconstituted by the replacement of the self-association region with a heterologous dimerisation domain. Intriguingly, we observed previously that $RPP_{139-297}$ undergoes MT-facilitated nuclear import, which is dependent on the DLC-AS (Moseley et al., 2007b). This indicates that the oligomeric state of the protein might regulate the nature of the interaction of RPP with MTs, providing a dynamic mechanism to modulate RPP nucleocytoplasmic trafficking. This is the first demonstration that a protein can harbour the capacity to undergo both MT-inhibited- and MT-facilitated nuclear import, indicating that the MT network has a more dynamic and important role in nucleocytoplasmic trafficking than previously thought. RPP also contains at least two NESs, an NLS in the globular CTD structure (Mavrakis et al., 2004; Moseley et al., 2007a; Pasdeloup et al., 2005), and, as shown here, a second sequence within the region 54-172 might effect nuclear accumulation of RPP (Fig. 3A). There are multiple phosphorylation sites in the RPP sequence (Fig. 1), and protein kinase C has been shown to regulate NES/NLS-mediated transport of the CTD (Moseley et al., 2007a), and might affect dimerisation or MT association, because several phosphorylation sites are found within RPP_{54-172} and in the CTD (Fig. 1). The high conservation of these trafficking and regulatory sequences among the P-proteins of rabies-virus-related lyssaviruses (Mavrakis et al., 2004) suggests that subcellular localisation of RPP is an essential and highly regulated aspect of viral pathogenicity.

In summary, we have identified a novel mechanism of IFN antagonism by human pathogenic virus, whereby a viral protein can alter the relationship of a transcription factor with the cytoskeleton and thereby affect its nuclear import and activation of transcription. Future research in our laboratory will focus on characterising the mechanism(s) regulating switching between the dual modes of RPP association with MTs and its potential as a target for antiviral drugs.

Materials and Methods

Constructs

RPP used in this study is derived from CVS-strain rabies virus. Constructs for the expression in mammalian cells of GFP-P1 (RPP_{1-297}), GFP-P3 (RPP_{54-297}), GFP-$RPP_{139-172}$, GFP-$RPP_{139-297}$, GFP-$RPP_{174-297}$, GFP-RPP_{1-172} and GFP-RPP_{54-172} were generated using PCR from the P1 DNA template and cloned in frame C-terminal to the GFP sequence of pEGFP-C1 or the mCherry sequence of pmCherry-C1 (Shaner et al., 2004) using a *Bam*HI-*Bgl*II strategy (Moseley et al., 2007a; Moseley et al., 2007b). P3 (D_{143}/Q_{147}-A) was produced by overlap PCR mutagenesis (Moseley et al., 2007a; Moseley et al., 2007b).

To produce GFP-Fv1-fused proteins, the coding sequence for Fv1 was PCR amplified from the pC4Fv1E vector (Ariad Pharmaceuticals, Cambridge, MA) and cloned into pEGFP-C1 in-frame C-terminal to the GFP sequence via the *Bam*HI-*Bgl*II cloning strategy to produce the pEGFP-Fv1 vector. Sequential *Bam*HI-*Bgl*II cloning (Moseley et al., 2007a; Moseley et al., 2007b) was performed to insert the coding sequences for $RPP_{139-172}$, $RPP_{139-297}$, $RPP_{139-297}(D_{143}/Q_{147}$-A) and $RPP_{174-297}$ into the pEGFP-Fv1 vector in-frame C-terminal to the GFP-Fv1 sequence.

The plasmid encoding STAT1-dsRed2 was a gift from Yi-Ling Lin, Institute of Biomedical Sciences, Academia Sinica, Taipei, Taiwan, Republic of China (Lin et al., 2006). The plasmid for expression of dynamitin-mCherry has been described previously (Roth et al., 2007). The plasmid for expression of α-tubulin mCherry was from the Tsien laboratory, Howard Hughes Medical Institute and Department of Pharmacology, University of California at San Diego, La Jolla, CA (Shaner et al., 2004).

Transfections, drug treatments and immunofluorescence

Cos7, HeLa, Vero, BSR and U-373-MG cells were cultured at 37°C, 5% CO_2 in DMEM medium with 10% FCS. For CLSM, cells were grown on coverslips to 80% confluency and transfected using Lipofectamine 2000 by the manufacturer's protocol, before live-cell CLSM as previously described (Alvisi et al., 2005; Moseley et al., 2007a; Moseley et al., 2007b; Roth et al., 2007). To disrupt or stabilise the MT network, cells were treated with NCZ (Sigma) for 4 hours at 5 μg/ml or TAX (Sigma) for 4 hours at 1 μg/ml (Moseley et al., 2007b; Roth et al., 2007). To activate IFN signalling for CLSM analysis, cells were treated with 2000 U/ml recombinant human IFNα (PML InterferonSource) or 3 ng/ml recombinant human IFNγ (Invitrogen) (added 2 hours before analysis). For inhibition of nuclear export mediated by CRM1, 2.8 ng/ml LMB (a gift from Minoru Yoshida, University of Tokyo, Tokyo, Japan) was added to cells for 4 hours before analysis.

For indirect immunofluorescence of tubulin, cells were fixed with 4% paraformaldehyde, before permeabilisation and labelling with anti-β-tubulin antibody (Cytoskeleton) followed by Alexa-Fluor-568-coupled secondary antibody (Invitrogen) as previously described (Moseley et al., 2007b; Roth et al., 2007). Alternatively, cells were fixed with methanol (10 minutes at –20°C) before labelling (Zhai et al., 1996). For indirect immunofluorescence of STAT1, cells were washed with PBS before fixation with 3.7% formaldehyde in PBS (10 minutes at room temperature) followed by 90% methanol (5 minutes at room temperature) before blocking (1% BSA, 2 hours, room temperature) and staining with anti-STAT1 (BD Biosciences, 610185) or anti-STAT1-*P* (Santa Cruz Biotechnology, sc-7988) followed by Alexa-Fluor-568-coupled secondary antibody (Invitrogen).

Confocal laser-scanning microscopy and image analysis

Routine CLSM for single-colour fluorophore live-cell analysis was performed using a Bio-Rad MRC-600 CLSM with a 40× water-immersion objective (NA 0.8) and heated stage (Alvisi et al., 2005; Lam et al., 2002; Moseley et al., 2007a; Moseley et al., 2007b; Poon et al., 2005; Roth et al., 2007); high-resolution CLSM was performed using an Olympus Fluoview 1000 with 60× oil-immersion lens (NA 1.4), and multicolour fluorophore imaging used the Olympus Fluoview 1000 (60× oil-immersion lens) or Leica SP5 (63× glycerol-immersion lens), with heated stage for live-cell imaging (Moseley et al., 2007b; Roth et al., 2007). In multicolour imaging, sequential scanning was performed to prevent cross-talk.

Analysis of digitised confocal files (single sections) was performed using ImageJ 1.62 public domain software (NIH) to calculate the ratio of nuclear to cytoplasmic fluorescence corrected for background (Fn/c) for individual cells; mean Fn/c values ± s.e.m. were calculated for samples of cells (n>30), and Graph Pad Instat software was used for statistical analysis, as previously described (Moseley et al., 2007a; Moseley et al., 2007b; Roth et al., 2007).

Dimerisation assays

To induce dimerisation of protein in live cells, we used the Ariad inducible homodimerisation kit (Ariad Pharmaceuticals, Cambridge, MA). Proteins containing the Fv1 inducible homodimerisation domain were expressed in Vero cells for 18-24 hours before addition of the cell-permeable dimerisation reagent (DR) AP20187 (Ariad) at a concentration of 100 nM for 1 hour before CLSM analysis as above.

MT association assay

MT and associated proteins were extracted from Cos-7 cells using the MT/Tubulin In Vivo Assay Kit (BK038, Cytoskeleton), as described (Davis et al., 2005). Cos7 cells transfected to express GFP-P3 and GFP-T-ag-NLS (residues 110-135 of the SV40 large-T antigen corresponding to the NLS) or GFP as negative controls, were lysed using MT stabilising buffer containing 100 μM GTP, 1 mM ATP, and 10 μl per ml of buffer of protease inhibitor cocktail for 10 minutes at 37°C. The lysates were subjected to ultracentrifugation (55,000 ***g*** for 30 minutes at 37°C) to separate the supernatant (containing soluble proteins and non-polymerised tubulin) from the MT fraction containing MT-associated proteins. Before resuspension, the pellet was washed three times. The fractions were analysed by western blotting using anti-GFP (1:1000, Roche) or anti-β-tubulin (1:500, Cytoskeleton) followed by HRP-linked secondary antibodies, before analysis using enhanced chemiluminescence (Perkin Elmer).

Luciferase assays and infections

For luciferase assays of IFN signalling, U-373-MG cells in 12-well plates were transfected with 0.75 μg pRL-TK and 2.5 μg pISREluc, with or without 2.5 μg plasmid encoding GFP, GFP-P3, GFP-Fv1 or GFP-Fv1-RPP$_{139-297}$. At 48 hours after transfection, cells were treated with or without 2000 U/ml IFN-α for 6 hours before harvesting and measurement of Firefly and *Renilla* luciferase activity according to the manufacturer's protocol (Dual-Luciferase Reporter Assay System; Promega). In some assays, cells were pretreated with NCZ (5 μg/ml added 1 hour before addition of IFN) and/or DR (100 nM for 1 hour before addition of IFN). Relative expression levels were calculated by dividing the Firefly luciferase values by those of the *Renilla* luciferase. In some cases, cells transfected with pRL-TK and pISREluc were infected 24 hours after transfection with rabies virus (CVS strain) at a multiplicity of infection (MOI) of 5 PFU/cell for 24 hours before treatment with IFN or NCZ as above.

This research was supported by the National Health and Medical Research Council, Australia (Project grant 384107, fellowship 384109). The authors acknowledge Ariad Pharmaceuticals (Cambridge, MA) for supplying the Ariad Inducible Homodimerisation Kit, Yi-Ling Lin for supplying the STAT1-dsRed2 vector, Roger Tsien for supplying the α-tubulin-mCherry vector and Minoru Yoshida for the gift of LMB. G.W.M. also acknowledges the staff of Monash Micro Imaging facility for their help and advice, and Cassandra David for support with cell culture.

References

Alvisi, G., Jans, D. A., Guo, J., Pinna, L. A. and Ripalti, A. (2005). A protein kinase CK2 site flanking the nuclear targeting signal enhances nuclear transport of human cytomegalovirus ppUL44. *Traffic* **6**, 1002-1013.

Billecocq, A., Spiegel, M., Vialat, P., Kohl, A., Weber, F., Bouloy, M. and Haller, O. (2004). NSs protein of Rift Valley fever virus blocks interferon production by inhibiting host gene transcription. *J. Virol.* **78**, 9798-9806.

Blondel, D., Regad, T., Poisson, N., Pavie, B., Harper, F., Pandolfi, P. P., De The, H. and Chelbi-Alix, M. K. (2002). Rabies virus P and small P products interact directly with PML and reorganize PML nuclear bodies. *Oncogene* **21**, 7957-7970.

Breakwell, L., Dosenovic, P., Karlsson Hedestam, G. B., D'Amato, M., Liljestrom, P., Fazakerley, J. and McInerney, G. M. (2007). Semliki Forest virus nonstructural protein 2 is involved in suppression of the type I interferon response. *J. Virol.* **81**, 8677-8684.

Brzozka, K., Finke, S. and Conzelmann, K. K. (2005). Identification of the rabies virus alpha/beta interferon antagonist: phosphoprotein P interferes with phosphorylation of interferon regulatory factor 3. *J. Virol.* **79**, 7673-7681.

Brzozka, K., Finke, S. and Conzelmann, K. K. (2006). Inhibition of interferon signaling by rabies virus phosphoprotein P: activation-dependent binding of STAT1 and STAT2. *J. Virol.* **80**, 2675-2683.

Campbell, E. M. and Hope, T. J. (2003). Role of the cytoskeleton in nuclear import. *Adv. Drug Deliv. Rev.* **55**, 761-771.

Chelbi-Alix, M. K., Vidy, A., El Bougrini, J. and Blondel, D. (2006). Rabies viral mechanisms to escape the IFN system: the viral protein P interferes with IRF-3, Stat1, and PML nuclear bodies. *J. Interferon. Cytokine Res.* **26**, 271-280.

Chenik, M., Chebli, K. and Blondel, D. (1995). Translation initiation at alternate in-frame AUG codons in the rabies virus phosphoprotein mRNA is mediated by a ribosomal leaky scanning mechanism. *J. Virol.* **69**, 707-712.

Davis, F. J., Pillai, J. B., Gupta, M. and Gupta, M. P. (2005). Concurrent opposite effects of trichostatin A, an inhibitor of histone deacetylases, on expression of alpha-MHC and cardiac tubulins: implication for gain in cardiac muscle contractility. *Am. J. Physiol. Heart Circ. Physiol.* **288**, H1477-H1490.

Dohner, K., Nagel, C. H. and Sodeik, B. (2005). Viral stop-and-go along microtubules: taking a ride with dynein and kinesins. *Trends Microbiol.* **13**, 320-327.

Gardner, K. H. and Montminy, M. (2005). Can you hear me now? Regulating transcriptional activators by phosphorylation. *Sci. STKE* **301**, pe44.

Ghildyal, R., Ho, A., Dias, M., Soegiyonom L., Bardin, P. G., Tran, K. C., Teng, M. N. and Jans D. A. (2009). The respiratory syncytial virus matrix protein possesses a Crm1-mediated nuclear export mechanism. *J. Virol.* **83**, 5353-5362.

Giannakakou, P., Sackett, D. L., Ward, Y., Webster, K. R., Blagosklonny, M. V. and Fojo, T. (2000). p53 is associated with cellular microtubules and is transported to the nucleus by dynein. *Nat. Cell Biol.* **2**, 709-717.

Gigant, B., Iseni, F., Gaudin, Y., Knossow, M. and Blondel, D. (2000). Neither phosphorylation nor the amino-terminal part of rabies virus phosphoprotein is required for its oligomerization. *J. Gen. Virol.* **81**, 1757-1761.

Haller, K., Rambaldi, I., Daniels, E. and Featherstone, M. (2004). Subcellular localization of multiple PREP2 isoforms is regulated by actin, tubulin, and nuclear export. *J. Biol. Chem.* **279**, 49384-49394.

Haller, O., Kochs, G. and Weber, F. (2006). The interferon response circuit: induction and suppression by pathogenic viruses. *Virology* **344**, 119-130.

Jans, D. A., Xiao, C. Y. and Lam, M. H. (2000). Nuclear targeting signal recognition: a key control point in nuclear transport? *BioEssays* **22**, 532-544.

Lam, M. H., Thomas, R. J., Loveland, K. L., Schilders, S., Gu, M., Martin, T. J., Gillespie, M. T. and Jans, D. A. (2002). Nuclear transport of parathyroid hormone (PTH)-related protein is dependent on microtubules. *Mol. Endocrinol.* **16**, 390-401.

Lillemeier, B. F., Koster, M. and Kerr, I. M. (2001). STAT1 from the cell membrane to the DNA. *EMBO J.* **20**, 2508-2517.

Lin, R. J., Chang, B. L., Yu, H. P., Liao, C. L. and Lin, Y. L. (2006). Blocking of interferon-induced Jak-Stat signaling by Japanese encephalitis virus NS5 through a protein tyrosine phosphatase-mediated mechanism. *J. Virol.* **80**, 5908-5918.

Malki, S., Berta, P., Poulat, F. and Boizet-Bonhoure, B. (2005). Cytoplasmic retention of the sex-determining factor SOX9 via the microtubule network. *Exp. Cell Res.* **309**, 468-475.

Mavrakis, M., McCarthy, A. A., Roche, S., Blondel, D. and Ruigrok, R. W. (2004). Structure and function of the C-terminal domain of the polymerase cofactor of rabies virus. *J. Mol. Biol.* **343**, 819-831.

Mikenberg, I., Widera, D., Kaus, A., Kaltschmidt, B. and Kaltschmidt, C. (2007). Transcription factor NF-kappaB is transported to the nucleus via cytoplasmic dynein/dynactin motor complex in hippocampal neurons. *PLoS ONE* **2**, e589.

Montgomery, S. A. and Johnston, R. E. (2007). Nuclear import and export of Venezuelan equine encephalitis virus nonstructural protein 2. *J. Virol.* **81**, 10268-10279.

Moseley, G. W., Filmer, R. P., DeJesus, M. A. and Jans, D. A. (2007a). Nucleocytoplasmic distribution of rabies virus P-protein is regulated by phosphorylation adjacent to C-terminal nuclear import and export signals. *Biochemistry* **46**, 12053-12061.

Moseley, G. W., Roth, D. M., DeJesus, M. A., Leyton, D. L., Filmer, R. P., Pouton, C. W. and Jans, D. A. (2007b). Dynein light chain association sequences can facilitate nuclear protein import. *Mol. Biol. Cell* **18**, 3204-3213.

Nishie, T., Nagata, K. and Takeuchi, K. (2007). The C protein of wild-type measles virus has the ability to shuttle between the nucleus and the cytoplasm. *Microbes. Infect.* **9**, 344-354.

Pasdeloup, D., Poisson, N., Raux, H., Gaudin, Y., Ruigrok, R. W. and Blondel, D. (2005). Nucleocytoplasmic shuttling of the rabies virus P protein requires a nuclear localization signal and a CRM1-dependent nuclear export signal. *Virology* **334**, 284-293.

Pemberton, L. F. and Paschal, B. M. (2005). Mechanisms of receptor-mediated nuclear import and nuclear export. *Traffic* **6**, 187-198.

Poisson, N., Real, E., Gaudin, Y., Vaney, M. C., King, S., Jacob, Y., Tordo, N. and Blondel, D. (2001). Molecular basis for the interaction between rabies virus phosphoprotein P and the dynein light chain LC8: dissociation of dynein-binding properties and transcriptional functionality of P. *J. Gen. Virol.* **82**, 2691-2696.

Poon, I. K. and Jans, D. A. (2005). Regulation of nuclear transport: central role in development and transformation? *Traffic* **6**, 173-186.

Poon, I. K., Oro, C., Dias, M. M., Zhang, J. and Jans, D. A. (2005). Apoptin nuclear accumulation is modulated by a CRM1-recognized nuclear export signal that is active in normal but not in tumor cells. *Cancer Res.* **65**, 7059-7064.

Randall, R. E. and Goodbourn, S. (2008). Interferons and viruses: an interplay between induction, signalling, antiviral responses and virus countermeasures. *J. Gen. Virol.* **89**, 1-47.

Rathinasamy, K. and Panda, D. (2008). Kinetic stabilization of microtubule dynamic instability by benomyl increases the nuclear transport of p53. *Biochem. Pharmacol.* **76**, 1669-1680.

Raux, H., Flamand, A. and Blondel, D. (2000). Interaction of the rabies virus P protein with the LC8 dynein light chain. *J. Virol.* **74**, 10212-10216.

Rawlinson, S. M., Pryor, M. J., Wright, P. J. and Jans, D. A. (2009). CRM1-mediated nuclear export of dengue virus RNA polymerase NS5 modulates interleukin-8 induction and virus production. *J. Biol. Chem.* **284**, 15589-15597.

Reich, N. C. and Liu, L. (2006). Tracking STAT nuclear traffic. *Nat. Rev. Immunol.* **6**, 602-612.

Roth, D., Moseley, G., Glover, D., Pouton, C. and Jans, D. (2007). A microtubule-facilitated nuclear import pathway for cancer regulatory proteins. *Traffic* **8**, 673-686.

Shaner, N. C., Campbell, R. E., Steinbach, P. A., Giepmans, B. N., Palmer, A. E. and Tsien, R. Y. (2004). Improved monomeric red, orange and yellow fluorescent proteins derived from Discosoma sp. red fluorescent protein. *Nat. Biotechnol.* **22**, 1567-1572.

Shaw, M. L., Garcia-Sastre, A., Palese, P. and Basler, C. F. (2004). Nipah virus V and W proteins have a common STAT1-binding domain yet inhibit STAT1 activation from the cytoplasmic and nuclear compartments, respectively. *J. Virol.* **78**, 5633-5641.

Shaw, M. L., Cardenas, W. B., Zamarin, D., Palese, P. and Basler, C. F. (2005). Nuclear localization of the Nipah virus W protein allows for inhibition of both virus- and toll-like receptor 3-triggered signaling pathways. *J. Virol.* **79**, 6078-6088.

Shimizu, K., Ito, N., Sugiyama, M. and Minamoto, N. (2006). Sensitivity of rabies virus to type I interferon is determined by the phosphoprotein gene. *Microbiol. Immunol.* **50**, 975-978.

Short, K. M., Hopwood, B., Yi, Z. and Cox, T. C. (2002). MID1 and MID2 homo- and heterodimerise to tether the rapamycin-sensitive PP2A regulatory subunit, alpha 4, to microtubules: implications for the clinical variability of X-linked Opitz GBBB syndrome and other developmental disorders. *BMC Cell Biol.* **3**, 1.

Vidy, A., Chelbi-Alix, M. and Blondel, D. (2005). Rabies virus P protein interacts with STAT1 and inhibits interferon signal transduction pathways. *J. Virol.* **79**, 14411-14420.

Vidy, A., El Bougrini, J., Chelbi-Alix, M. K. and Blondel, D. (2007). The nucleocytoplasmic rabies virus P protein counteracts interferon signaling by inhibiting both nuclear accumulation and DNA binding of STAT1. *J. Virol.* **81**, 4255-4263.

Yamasaki, C., Tashiro, S., Nishito, Y., Sueda, T. and Igarashi, K. (2005). Dynamic cytoplasmic anchoring of the transcription factor Bach1 by intracellular hyaluronic acid binding protein IHABP. *J. Biochem.* **137**, 287-296.

Zhai, Y., Kronebusch, P. J., Simon, P. M. and Borisy, G. G. (1996). Microtubule dynamics at the G2/M transition: abrupt breakdown of cytoplasmic microtubules at nuclear envelope breakdown and implications for spindle morphogenesis. *J. Cell Biol.* **135**, 201-214.

Ziegler, E. C. and Ghosh, S. (2005). Regulating inducible transcription through controlled localization. *Sci. STKE* **2005**, re6.